Classification: BIOLOGICAL SCIENCES, Immunology.

**AID-induced decrease in topoisomerase 1 induces DNA structural alteration and DNA cleavage for class switch recombination**

Maki Kobayashi[*], Masatoshi Aida[*], Hitoshi Nagaoka, Nasim A. Begum, Yoko Kitawaki, Mikiyo Nakata, Andre Stanlie, Tomomitsu Doi, Lucia Kato, Il-mi Okazaki[†], Reiko Shinkura, Masamichi Muramatsu[§], Kazuo Kinoshita[‡], and Tasuku Honjo

Department of Immunology and Genomic Medicine, Graduate School of Medicine, Kyoto University, Yoshida Sakyo-ku, Kyoto 606-8501, Japan

[†]Present address: Division of Immune Regulation, Institute for Genome Research, The University of Tokushima, 3-18-15 Kuramoto, Tokushima, 770-8503, Japan

[§]Present address: Department of Molecular Genetics, Graduate School of Medical Science, Kanazawa University, 13-1 Takara-machi, Kanazawa 920-8640, Japan

[‡]Present address: Evolutionary Medicine, Shiga Medical Center Research Institute, 5-4-3 Moriyama, Moriyama-City, Shiga 524-8524, Japan

[*] These authors contributed to this work equally.

Corresponding author: Tasuku Honjo; Phone +81-75-753-4371; Fax +81-75-753-4388; E-mail honjo@mfour.med.kyoto-u.ac.jp

Manuscript information: 23 pages; 6 Figures; 9 Supplementary Figures; 2 Supplementary Tables; 2 Supplementary Information.

**Abstract**

**To initiate class switch recombination (CSR) activation-induced cytidine deaminase (AID) induces staggered nick cleavage in the S region which lies 5' to each immunoglobulin constant region gene and rich in palindromic sequences. Topoisomerase 1 (Top1) controls the supercoiling of DNA by nicking, rotating, and religating one strand of DNA. Curiously, Top1 reduction or AID overexpression causes the genomic instability. Here we report that the inactivation of Top1 by its specific inhibitor camptothecin drastically blocked both the S region cleavage and CSR, indicating that Top1 is responsible for the S region cleavage in CSR. Surprisingly, AID expression suppressed Top1 mRNA translation and reduced its protein level. In addition, the decrease in the Top1 protein by RNA-mediated knockdown augmented the AID-dependent S region cleavage as well as CSR. Furthermore, Top1 reduction altered DNA structure of the Sμ region. Taken together, AID-induced Top1 reduction alters S region DNA structure probably to non-B form, on which Top1 can introduce nicks but cannot religate, resulting in S region cleavage.**

¥body

**Introduction**

Class switching is one of the critical features of antibody memory that is required for vaccination. Class switching is accomplished by region-specific recombination between two switch (S) regions located upstream of the immunoglobulin (Ig) heavy-chain constant region ($C_H$) gene (1, 2). Class switch recombination (CSR) is a unique type of recombination distinct from site-specific, homologous or illegitimate recombination because the S region consists of tandem arrays of repetitive sequences rich in inverted repeats or palindromes. Such sequences facilitate formation of stem-loop, cruciform and other non-B DNA structures (3).

Transcription of the S region is initiated from the I promoter that is specific to each S region, and is essential to trigger CSR (4, 5). The S region transcripts seem to remain on the DNA template for a short period, thus facilitating the formation of R-loop. Lieber and his colleagues reported that the bisulfite treatment of nuclear DNA from switch-induced spleen cells converted dC to dU in the Sμ region, indicating the presence of single stranded DNA in the Sμ region in activated B cells (6, 7). R-loop may not survive long but lead to the formation of non-B structures including stem-loop, cruciform, and triplex in the S region because of abundant inverted repeats (3, 8-10).

Frequent and long deletions and duplications are observed at the CSR junctions in artificial switch substrates designed to select inversion-type products (11). The results suggest that the double strand breaks (DSBs) in the S regions leading to CSR, are generated by the staggered nick-type cleavages because deletions and duplications are most likely to be generated during

the repair of staggered nicked ends with single-strand overhangs by exonucleases or DNA polymerases.

AP endonuclease 1 and 2 (Apex 1 and 2) and topoisomerase 1 (Top1) represent evolutionally conserved nicking enzymes. Apex1 and 2 cleave abasic sites generated by base excision enzymes such as uracil DNA glycosylase, which are proposed to be involved in CSR (12, 13). However, we have shown that both Apex1 and 2 are not essential for CSR (14). Top1 reduces excessive supercoiling in the DNA of mammalian cells (15). It binds to DNA, cleaves one strand and fixes the 3' phosphate of the cleaved end by forming a transient covalent bond with its tyrosine residue. The transient complex is quickly resolved by re-ligation after rotating the non-fixed end of the DNA strand around the helical axis. A specific inhibitor of Top1, camptothecin (CPT) can be intercalated into this transient cleavage complex of Top1 and DNA to block Top1's catalytic function while CPT does not affect free Top1(16). Curiously, the reduction of Top1 by RNA mediated knockdown in cultured cells causes the genome-wide instability (17). Activation-induced cytidine deaminase (AID) is essential for CSR and involved in S region cleavage, but its molecular mechanism is unknown (12, 13, 18, 19). AID has two functions in CSR: one for S region cleavage and the other for the end joining step (20). Interestingly, AID introduces DNA cleavage in multiple genetic loci, resulting in the genome instability (20-23).

We found that CPT almost completely inhibited CSR and DNA cleavage in the S region induced by AID, indicating that Top1 is the major, if not a sole, nicking enzyme in CSR. We then found that AID expression reduced the Top1 protein amount primarily by suppression of Top1 mRNA translation. In addition, Top1 reduction altered the Sμ region structure, which

probably prevents the rotation and religation steps after cleavage by Top1. From these observations, we propose a model that S region cleavage is due to suppression of religation by Top1 on non-B DNA which is formed by inefficient relaxation of transcription-coupled supercoiling because of Top1 reduction by AID.

## Results

### Top1 inhibition by CPT blocks CSR

Since Apex1 and 2 are not required for CSR (14), we suspected involvement of Top1. We thus tested the effect on CSR of treating cells with CPT that specifically stabilizes the Top1-DNA intermediate complex and inhibits the catalytic function of Top1. The IgA switching of CH12F3-2 cells 24 hours after stimulation with a mixture of CD40L, IL-4, TGFβ (CIT) was reduced in the presence of CPT in a dose dependent manner (Fig. 1A). CPT (60nM) inhibited CSR to 13% while 80% of cells remained alive even after 24 hours. The inhibition of CSR was more directly demonstrated by a drop in α circle transcripts (αCT) which are transcribed from looped-out circular DNA (24) (Fig. S1A). The drop in αCT by increment of CPT paralleled the reduction of IgA expression. We also confirmed that this strong blockade of CSR by CPT was not due to the suppression of either AID expression or germline transcription of the Sμ and Sα regions in CH12F3-2 cells (Fig. S1B).

The inhibition of CSR by CPT was confirmed in splenic B cells. AID deficient splenic B cells were stimulated by LPS and IL-4, and infected with the retrovirus expressing AID fused with the hormone binding domain of the estrogen receptor (ER) (AIDER) (25). AIDER was then activated by the addition of tamoxifen (4-OHT) 24 hours after the infection. The surface expression of IgG1 in splenic B cells was inhibited by 30 or 60nM CPT (Fig. 1B). To examine the effect of CPT more quickly, we performed the digestion circularization (DC) PCR method (26). As early as 3 or 6 hours after the activation of AIDER with 4-OHT, we could already detected Sγ1-Sμ DC-PCR products of Sγ1-Sμ recombination which results from recombination between the Sγ1 and Sμ regions (Fig. 1C and Fig. S1C). The amount of Sγ1-Sμ DC-PCR products was drastically reduced by 3-hour incubation with 30nM or 60nM

CPT, indicating that the blockage of CSR by CPT is unlikely to be the secondary effect of cell death. None of Top2α inhibitors blocked CSR as assessed by αCT synthesis (Table S1).

**CPT inhibits S region DNA cleavage**

To assess whether CPT inhibits DNA cleavage in the S region, we first examined the γH2AX focus formation in the S region. A chromatin immunoprecipitation (CHIP) assay using anti-γH2AX antibodies clearly showed that γH2AX accumulated in the Sμ region and Cμ exons but not in the *Gapdh* or *Icos loci* in response to DNA cleavage in AER cells *i.e.* CH12F3-2 cell expressing AIDER following the addition of 4-OHT as reported previously (Fig. 2A) (27). γH2AX focus formation at the Sμ region and Cμ exons was severely blocked by 50nM CPT, indicating that CPT suppresses AID-induced DSBs in the Sμ region.

Using semi-quantification of DSBs ends by ligation of a biotinylated linker, we confirmed that the number of DSBs of the Sμ and Sα region was clearly reduced in AER cells by 10 and 30 nM CPT (Fig. 2B). On the other hand, the Sγ1 region cleavage was not affected by CPT. Also, although 150nM CPT induced numerous non-specific DNA cleavage, it did not induce a significant number of such cleavage below 50nM used in the present study (Fig. S2). Finally, since CPT, a substrate-enzyme intercalating inhibitor of Top1, blocks the AID-induced DSBs of the S region at concentrations far below CPT's $IC_{50}$ (ca 7μM) (28), the S region might be preferred target to Top1. These results demonstrate that Top1 is the enzyme responsible for DNA cleavage during AID-induced CSR.

**AID expression reduces Top1 protein**

We then explored a possible relationship between Top1 and AID. We compared the Top1

protein level between wild-type and AID deficient splenic B cells stimulated with LPS and IL-4 (Fig. 3A). Surprisingly, 24 hours after stimulation the wild-type splenic B cells showed a decreased level of the Top1 protein that was about 60% of the level in the non-stimulated or AID deficient spleen cells. When we introduced retrovirus carrying AIDER into the AID deficient splenic B cells, wild-type AIDER expression reduced the Top1 protein to 50% 3 hours after 4-OHT stimulation compared with expression of a catalytically inactive mutant of AIDER (KSS) (Fig. 3B). This faster reduction of the Top1 protein is probably because of the rapid activation of the accumulated AIDER by 4-OHT.

When AER cells were stimulated with 4-OHT or CIT, the Top1 protein was also reduced but more slowly (Fig. S3A) probably because cell lines proliferate much faster and thus contain a much larger amount of the Top1 protein than splenic B cells (unpublished data). The majority of the Top1 protein is localized in nucleoli and the turnover of the nucleolar Top1 protein is much slower than the nucleoplasmic Top1 (29, 30). We therefore quantified the Top1 protein level in the nucleoplasmic fraction of AER cells after the addition of 4-OHT and found that the Top1 amount was reduced quickly (Fig. 3C). Similarly, NIH3T3 fibroblasts expressing AIDER but not its KSS mutant decreased the Top1 protein amount in the nucleoplasm fraction following 4-OHT stimulation (Fig. S3B). We also found that C-terminally truncated AID (Jp8Bdel) also reduced Top1 protein (Fig. S3C). (20). The mRNA level of Top1 was decreased by around 20% 48 hours after stimulation of splenic B or CH12F3-2 cells (Fig. S3D). We therefore suspected that the reduction in the Top1 protein was mostly due to either the suppression of Top1 mRNA translation or to enhanced degradation of the Top1 protein.

**AID suppresses the translation of Top1 mRNA**

We first determined the half life of the Top1 protein in AER cells to be 3.7 hours by the addition of cycloheximide (CHX) (Fig. 4A). The half-life of the Top1 protein was not shortened significantly by AID activation, indicating that AID does not accelerate the degradation of Top1. We then directly examined whether Top1 protein synthesis is reduced by AID induction. AID activation clearly suppressed the rate of the Top1 protein synthesis to a half while the total protein synthesis is not affected (Fig. 4B and Fig.S4). We sequenced the Top1 cDNA in AID expressing B cells and found no mutations in either the coding or 3' UTR sequence (Fig. S5). Therefore, Top1 mRNA does not seem to be a direct editing target of AID. The half life (3.7 hours) and translation reduction rate (0.5) well explains experimental reduction of Top1 protein (see Discussion). Collectively, these results suggest that the Top1 reduction induced by AID activation was caused primarily by the suppression of Top1 mRNA translation and less significantly by Top1 mRNA degradation.

**Top1 knockdown enhances CSR**

We then examined whether a Top1 reduction induced by AID is functionally relevant to CSR. Small interfering (si)RNA oligos to Top1 mRNA were introduced into AER cells to knock down the Top1 protein, and their effects on CSR were examined. Two Top1 siRNA oligos (No. 33 and 35) knocked down the Top1 protein strongly in AER cells although measurable amounts of Top1 always remained (Fig. 5A). Surprisingly, the Top1 protein knockdown by either of the Top1 siRNA oligos clearly augmented CSR induced by various levels of AID activation, which was controlled by changing the concentrations of either CIT or 4-OHT (Fig. 5B). The magnitude of CSR augmentation by Top1 reduction was greater in the 4-OHT activated AER cells than in the CIT-activated cells probably because 4-OHT caused lower

AID activation than did CIT as evidenced by a lower efficiency of IgA switching and stronger inhibition by AID knockdown. The augmentation of CSR by the Top1 knockdown was not due to an increase in Iμ and Iα germline transcription, or endogenous AID expression in AER cells with or without 4-OHT stimulation (Fig. S6A).

We also generated AER cell lines containing plasmids carrying tetracycline (Tet) - inducible microRNA directed to Top1 mRNA or a randomized negative control. In this cell line, CSR was gradually augmented in parallel with Top1 knockdown by increasing expression of the Top1-directed microRNA but not the negative control (Fig. 5C, left panel and Fig. S6B). The augmentation of CSR by Top1 knockdown was also dependent on AIDER activation by 4-OHT (Fig. 5C, right panel). A slight increase in CSR by Top1 knockdown was observed without 4-OHT, which might have been due to the basal level of AID expression in CH12F3-2 cells. CSR enhancement by Top1 knockdown was also obvious in splenic $AID^{-/-}$ B cells that were electroporated to incorporate Top1 siRNA and then infected by AIDER retrovirus, followed by 4-OHT activation (Fig. 5D and Fig. S6C).

**Top1 knockdown enhances S region cleavage**

We then asked whether Top1 reduction stimulated DNA cleavage in the S region. When the Top1 protein was decreased by either Top1 siRNA No. 33 or No. 35, the DSBs were strongly increased in the Sμ and Sα regions but not the Sγ1 region in AER cells compared with AER cells treated with control siRNA (Fig. 2C). Similarly, the Top1 knockdown by the Tet-inducible microRNA in AER cells also enhanced cleavage in the Sμ but not the Sγ1 region (Fig. 2D). Thus, we concluded that Top1 reduction facilitates CSR by enhancing the S region cleavage. Importantly, the DSBs that were augmented by the Top1 knockdown were

also inhibited by 25 and 50 nM CPT, indicating that DNA cleavage augmented by Top1 reduction is also catalyzed by Top1 (Fig. 2E).

**Top1 knockdown induces structural changes in the S region**

To explore the mechanism by which AID-mediated Top1 reduction augments S region cleavage and CSR, we speculated that aberrant supercoiling by Top1 protein reduction may induce non-B DNA structure in the S region so that Top1 cannot religate, resulting in irreversible cleavage by Top1. DNA structural alterations can be estimated by the DNA's sensitivity to bisulfite modification from dC to dU which occurs in the single-stranded regions (6, 7). The presence of consecutive C bases is suitable for determining the single-strandedness by the bisulfite assay (7). We found that the three major C clusters (Fig. 6A and B; I, II and III) within the 150bp region 3' to the core Sμ region in CH12F3-2 cells showed a higher sensitivity to the bisulfite treatment following Top1 knockdown. A similar increase in bisulfite sensitivity was observed in the same clusters following CIT stimulation. Since the Sμ locus is transcriptionally active in CH12F3-2 cells, we observed about a 16% basal reactivity estimated by the total conversion frequency (Fig. 6C), which was increased to 27% upon Top1 knockdown. These results suggest that Top1 reduction indeed affected the DNA structure of the Sμ region. Although Top1 normally cleaves and re-ligates one strand of DNA, when Top1 levels are reduced, structural alterations in the S region may form non-B structures that block the rotation and religation step, resulting in irreversible cleavage by Top1.

**Discussion**

In the present study, we showed that CPT an intercalating inhibitor of the Top1 catalytic activity (15, 16) blocked both CSR and S region cleavage induced by AID activation in B cells. In addition, AID expression reduced the Top1 protein amount by suppression of Top1 mRNA translation. This activity of AID depends on its deamination activity but not on the C-terminal domain that is not required for DNA cleavage (20). Furthermore, Top1 reduction mediated by RNA knockdown enhanced AID-induced CSR and S region DNA cleavage. From these observations, we conclude that the activation of AID reduces the Top1 protein and this decrease in the Top1 protein enhances DNA cleavage in the S region. CPT also inhibited DSBs augmented by Top1 knockdown. It is therefore likely that Top1 is the enzyme that introduces the DSBs by staggered nick cleavage in the S region after AID activation in B lymphocytes.

The mechanism by which Top1 introduces DSBs requires inhibition of the religation step of Top1. Transcription elongation by RNA polymerase II introduces uneven DNA supercoiling leading to a positive supercoil in the front of the migrating transcriptional machinery and negative supercoil at the rear. Top1 reduction is likely to retard relaxation of negative supercoil. Excessive negative supercoil of DNA facilitates local structural alterations including R-loop, stem-loop, cruciform, triplex and other non-B DNA structures in DNA rich in palindromes or G/C stretches like the S region, which probably inhibits the religation step of Top1 after cleavage. (3, 8-10) (Fig. S7, 8). In addition, Top1 phosphorylates and activates the alternative splicing factor ASF/SF2 (31). Thus, it is possible that Top1 protein reduction may disturb splicing of S region transcripts and prolong the half life of S region transcripts, leading to the formation of frequent R-loop and consequent non-B DNA structures in the S

region (3, 32). In support of this hypothesis, the reduction of either Top1 or ASF induces genomic instability (17, 32). In fact, we observed that the single stranded fraction of the Sμ region was augmented by Top1 knockdown. Interestingly, a similar bisulfite reactivity pattern was observed at the chromosomal instability sites identified in the bcl-2 and c-myc loci (8, 9).

Furthermore, Top1 promotes the formation of G-quartet structures and binds to non-B forms of DNA such as cruciform and G-quartet DNA, which can occur in G-rich single-stranded regions (33, 34). Non-B form structures may result in irreversible cleavage on either strand of the S region by Top1 because the DNA rotation around the helix may be disturbed after nicking, thus inhibiting the Top1's religation activity (Fig. S8). In other words, the Top1 reduction may induce the structural changes of the S regions that favor irreversible cleavage by Top1.

Given the half-life of 3.7 hours and reduction rate of translation to 50%, the Top1 protein level at a given time point (t in hour) after initiation of translation reduction is equal to $0.5\ A_0\ (1+e^{-0.187t})$ where $A_0$ is the initial amount of Top1 protein. This equation predicts that the Top1 protein amount converges to a half about 24 hours after initiation of translation reduction. The experimental results are in general agreement with this prediction. How can Top1 mRNA translation be modulated by AID? Since the Top1 mRNA is not directly edited, we speculate that AID may edit small molecular weight RNA such as microRNAs that change the target specificity to regulate Top1 mRNA translation (Fig. S9). In summary, we have shown that Top1 is involved in the DNA cleavage step of CSR although the details of the mechanism remain to be explored.

**Materials and Methods**

All data shown are representatives of at least three experiments.

**Knockdown of Top1**

*siRNA system:*TopI siRNA #33 or #35, or a low GC control RNA (all by Invitrogen) were electroporated into CH12F3-2, AER or splenic B cells and incubated for 24 hours before stimulation. *miR system:* miR-Top1 was designed by BLOCK-iT™ RNAi Designer (Invitrogen), and cloned into pcDNA™6.2-GW/EmGFP-miR (Invitrogen). pcDNA™6.2-GW/EmGFP/miR-neg control (miR-neg) plasmid was used as the negative control. The sequences of miR and siRNA are in Table S2. *Tet-ON system:* AER cells was transduced by pLenti6/TR (Invitrogen) and selected with 5 μg/ml of blasticidin to get the Tet repressor positive (TetR+) subclone. pCMV promoter of the miR vectors was substituted by Tet operator promoter from pcDNA™4/TO/LacZ (Invitrogen). The TetR+ cells were electroporated by the Tet-operative miR vector, sorted by flow cytometry and subcloned. In the experiments, the cells were exposed to Tet or dox for 24 hours before AID activation.

**DNA Break Assay by Biotinylated Linker-ligation**

Biotinylated linker-ligation method is based on biotinylated dUTP method (20). DNA break site is blunted and ligated with biotinylated linker. Sonicated labeled DNA were trapped with streptavidin magnetic beads, followed by second linker ligation. DNA was further globally amplified with linker-specific primers, and purified with WIZARD SV Gel and PCR Reaction Clean-up system (Promega). Gene-locus specific quantitative PCR was performed with ABI 7900HT. 4% of total the sample was taken as the input DNA, just before trapping by magnetic beads. *Sμ*, *Sα*, or *Sγ1* locus signal, calculated by beads-bound/input, is further standardized by the signal (beads-bound/input) of *β2-microglobulin* locus or *β-actin* locus to compensate the

recovery of beads and DNA. All the sequences of linkers and oligos were described in Table S2.

**Metabolic Labeling of Newly Synthesized Proteins**

Newly synthesized protein was labeled with Click-iT AHA for Nascent Protein Synthesis kit and Click-iT Biotin Protein Analysis Detection Kit (invitrogen) according to manufacturer's instructions. One million AER cells were labeled with 500 μM of AHA for indicated times and lysed in the lysis buffer (50 mM Tris-HCl pH8.0, 1% SDS and 1x Complete (Roche), 2.5kU/ml Benzonase (Novagen)). AHA incorporated protein was biotinylated. After precipitation and dissolving, biotinylated protein was collected with Dynabeads M-280 (Invitrogen). Protein was eluted into SDS sample buffer by boiling and quantified by Western blot with αTopI antibody. Total protein biotinylation efficiency was measured by dot blot onto the nitrocellulose membrane. After blocking, the membrane was incubated with HRP-conjugated, streptavidin-labeled antibody, washed and colored by chemi-luminescence.

**Bisulfite Modification of Genomic DNA**

CH12F3-2 cells were either stimulated with CIT or left untreated 24 hours after siRNA (GC-control and Top1) introduction, incubated for another 24 hours and harvested for surface IgA expression assay and genomic DNA isolation. Genomic DNA bisulfite modification of the Sμ region was carried out as previously described with some modifications (7). High molecular weight genomic DNA was isolated using Qiagen genomic DNA isolation system and processing of bisulfite modified DNA was performed following the instruction of Bisulfite modification system (Human Genetic Signatures). Amplification of the sequence 3' to the Sμ core region with FTH111 and FTH94 primers.

Materials and other conventional experimental procedures are described in Supporting Information.

**Acknowledgement**

The authors are grateful to Ms. Y. Shiraki and T. Kanda for the preparation of the manuscript. This research was supported by a Grant-in Aid for Specially Promoted Research 17002015 and also by Global COE Program of the Ministry of Education, Culture, Sports, Science and Technology (MEXT), Japan.

**References**


1. Honjo T, Kinoshita K, Muramatsu M (2002) Molecular mechanism of class switch recombination: linkage with somatic hypermutation. *Annu Rev Immunol* 20:165-196.
2. Stavnezer J, Guikema JE, Schrader CE (2008) Mechanism and regulation of class switch recombination. *Annu Rev Immunol* 26:261-292.
3. Wells RD (2007) Non-B DNA conformations, mutagenesis and disease. *Trends Biochem Sci* 32:271-278.
4. Yancopoulos GD*, et al.* (1986) Secondary genomic rearrangement events in pre-B cells: VHDJH replacement by a LINE-1 sequence and directed class switching. *Embo J* 5:3259-3266.
5. Stavnezer-Nordgren J, Sirlin S (1986) Specificity of immunoglobulin heavy chain switch correlates with activity of germline heavy chain genes prior to switching. *Embo J* 5:95-102.
6. Roy D, Yu K, Lieber MR (2008) Mechanism of R-loop formation at immunoglobulin class switch sequences. *Mol Cell Biol* 28:50-60.
7. Huang FT*, et al.* (2007) Sequence dependence of chromosomal R-loops at the immunoglobulin heavy-chain Smu class switch region. *Mol Cell Biol* 27:5921-5932.
8. Tsai AG*, et al.* (2009) Conformational variants of duplex DNA correlated with cytosine-rich chromosomal fragile sites. *J Biol Chem* 284:7157-7164.
9. Raghavan SC*, et al.* (2005) Evidence for a triplex DNA conformation at the bcl-2 major breakpoint region of the t(14;18) translocation. *J Biol Chem* 280:22749-22760.
10. Collier DA, Griffin JA, Wells RD (1988) Non-B right-handed DNA conformations of homopurine.homopyrimidine sequences in the murine immunoglobulin C alpha switch region. *J Biol Chem* 263:7397-7405.
11. Chen X, Kinoshita K, Honjo T (2001) Variable deletion and duplication at recombination junction ends: implication for staggered double-strand cleavage in class-switch recombination. *Proc Natl Acad Sci U S A* 98:13860-13865.
12. Rada C*, et al.* (2002) Immunoglobulin isotype switching is inhibited and somatic hypermutation perturbed in UNG-deficient mice. *Curr Biol* 12:1748-1755.
13. Petersen-Mahrt SK, Harris RS, Neuberger MS (2002) AID mutates E. coli

suggesting a DNA deamination mechanism for antibody diversification. *Nature* 418:99-103.

14. Sabouri Z, *et al.* (2009) Apex2 is required for efficient somatic hypermutation but not for class switch recombination of immunoglobulin genes. *Int Immunol* 21:947-955.
15. Pommier Y (2006) Topoisomerase I inhibitors: camptothecins and beyond. *Nat Rev Cancer* 6:789-802.
16. Kerrigan JE, Pilch DS (2001) A structural model for the ternary cleavable complex formed between human topoisomerase I, DNA, and camptothecin. *Biochemistry* 40:9792-9798.
17. Miao ZH, *et al.* (2007) Nonclassic functions of human topoisomerase I: genome-wide and pharmacologic analyses. *Cancer Res* 67:8752-8761.
18. Muramatsu M, *et al.* (2000) Class switch recombination and hypermutation require activation-induced cytidine deaminase (AID), a potential RNA editing enzyme. *Cell* 102:553-563.
19. Revy P, *et al.* (2000) Activation-induced cytidine deaminase (AID) deficiency causes the autosomal recessive form of the Hyper-IgM syndrome (HIGM2). *Cell* 102:565-575.
20. Doi T, *et al.* (2009) The C-terminal region of activation-induced cytidine deaminase is responsible for a recombination function other than DNA cleavage in class switch recombination. *Proc Natl Acad Sci U S A* 106:2758-2763.
21. Okazaki IM, *et al.* (2003) Constitutive expression of AID leads to tumorigenesis. *J Exp Med* 197:1173-1181.
22. Liu M, *et al.* (2008) Two levels of protection for the B cell genome during somatic hypermutation. *Nature* 451:841-845.
23. Ramiro AR, *et al.* (2006) Role of genomic instability and p53 in AID-induced c-myc-Igh translocations. *Nature* 440:105-109.
24. Kinoshita K, Harigai M, Fagarasan S, Muramatsu M, Honjo T (2001) A hallmark of active class switch recombination: transcripts directed by I promoters on looped-out circular DNAs. *Proc Natl Acad Sci U S A* 98:12620-12623.
25. Doi T, Kinoshita K, Ikegawa M, Muramatsu M, Honjo T (2003) De novo protein synthesis is required for the activation-induced cytidine deaminase function in class-switch recombination. *Proc Natl Acad Sci U S A* 100:2634-2638.

26. Chu CC, Paul WE, Max EE (1992) Quantitation of immunoglobulin mu-gamma 1 heavy chain switch region recombination by a digestion-circularization polymerase chain reaction method. *Proc Natl Acad Sci U S A* 89:6978-6982.
27. Petersen S*, et al.* (2001) AID is required to initiate Nbs1/gamma-H2AX focus formation and mutations at sites of class switching. *Nature* 414:660-665.
28. Scaldaferro S, Tinelli S, Borgnetto ME, Azzini A, Capranico G (2001) Directed evolution to increase camptothecin sensitivity of human DNA topoisomerase I. *Chem Biol* 8:871-881.
29. Christensen MO*, et al.* (2004) Distinct effects of topoisomerase I and RNA polymerase I inhibitors suggest a dual mechanism of nucleolar/nucleoplasmic partitioning of topoisomerase I. *J Biol Chem* 279:21873-21882.
30. Muller MT, Pfund WP, Mehta VB, Trask DK (1985) Eukaryotic type I topoisomerase is enriched in the nucleolus and catalytically active on ribosomal DNA. *Embo J* 4:1237-1243.
31. Eisenreich A*, et al.* (2009) Cdc2-like kinases and DNA topoisomerase I regulate alternative splicing of tissue factor in human endothelial cells. *Circ Res* 104:589-599.
32. Li X, Manley JL (2005) Inactivation of the SR protein splicing factor ASF/SF2 results in genomic instability. *Cell* 122:365-378.
33. Arimondo PB*, et al.* (2000) Interaction of human DNA topoisomerase I with G-quartet structures. *Nucleic Acids Res* 28:4832-4838.
34. Thiyagarajan MM, Waldman SA, Noe M, Kmiec EB (1998) Binding characteristics of Ustilago maydis topoisomerase I to DNA containing secondary structures. *Eur J Biochem* 255:347-355.

**Figure Legends**

**Figure 1. CPT blocks CSR in CH12F3-2 cells and splenic B cells. A.** The percentages of the $IgA^+$ and propidium iodide $(PI)^-$ alive cells are presented as closed and open circles, respectively. Each circle represents average with S.D. (n=3). The backgrounds (subtracted) of $IgA^+$ and $PI^+$ cells at 0 nM CPT were 1.26% and 11.5%, respectively. **B.** $AID^{-/-}$ spleen cells were

infected by AIDER-IRES-GFP retrovirus. 24 hours later, the cells were treated with 1 μM 4-OHT or EtOH in the presence of 30 to 60 nM CPT. After an additional 24-hour incubation, surface IgG1 and GFP expression were analyzed by flow cytometry with biotinylated anti-IgG1 antibody and streptavidin-APC. The percentage of IgG1 switch in the GFP positive cells is shown above each plot. Mock, no retrovirus control. **C.** *Sγ1-Sμ* DC-PCR. Prior to the flow cytometry in panel B, part of cells were collected 3 and 6 hours after 4-OHT and CPT addition. Extracted genomic DNA was then subjected to DC-PCR for the *Sγ1-Sμ* recombination (*γ1-μ*) and for the nicotinic acetylcholine receptor (*nAchR*) locus as control. PCR products were run on a 2% agarose gel and visualized by ethidium bromide.

**Figure 2. CPT inhibits the DNA cleavage in CSR. A.** AER cells were cultured with 50 nM CPT for 12 hours then stimulated with CIT and 1μM 4-OHT. Cells were harvested 8 hours after the stimulation and γH2AX accumulation at the indicated gene loci was assessed by CHIP. Cells treated with 0.5 μM staurosporin were shown as a positive control. A numeric value representing the non-specific IgG precipitation was subtracted as a background. The graph represents the average of 4 independent experiments with a standard deviation. **B-E.** DNA break assay was carried out as described in Materials and Methods. Indicated concentrations of CPT were added at the same time as 4-OHT (1 μM). **B.** CPT effect on DNA break induced by AID. AER cells were stimulated for 16 hours with 4-OHT. **C.** Top1 knockdown was carried out for 24 hours with siRNA oligo #33 or #35 in AER cells. Cells were harvested 24 hours later from the start of 4-OHT. **D.** Knockdown of Top1 in AER cells was carried out by miR expression with 50 ng/ml tetracycline (Tet). AER cells were activated for 24 hours by 1 μM 4-OHT. AER cells with microRNA-negative control (miR-neg) were used as control. **E.** AER cells with Top1 knockdown by siRNA oligo #33 for 24 hours and

subsequently stimulated.

**Figure 3. Top1 protein is decreased by AID expression. A-C.** The protein amounts were measured by Western blotting using appropriate antibodies. **A.** Wild type (W) and $AID^{-/-}$ ($A^{-/-}$) splenic B cells were stimulated for the indicated periods by LPS and IL-4. The relative Top1 protein amounts normalized by tubulin are plotted at the right. **B.** $AID^{-/-}$ mouse splenic B cells were infected by retroviruses carrying AIDER (W) or its KSS-mutant (K). 4-OHT (1 μM) was added 24 hours after infection. Relative Top1 protein levels at indicated time points after 4-OHT addition are plotted as above. **C.** Top1 protein levels in the nucleoplasm fraction of AER cells at indicated time points after 4-OHT addition were measured, normalized by lamin, and are plotted as above.

**Figure 4. AID reduces the Top1 protein level by inhibiting its translation. A.** Half-life of Top1. AER cells were treated with 50 μM Z-VAD-FMK, 1 μM of 4-OHT and 10 μg/ml of CHX at the indicated time points. Whole cell extract was collected serially, and Top1 was measured by Western blot and plotted. **B.** Translation rate of Top1. AER cells were cultured in methionine free medium with or without 1 μM 4-OHT for one hour before L-azidohomoalanine (AHA) addition at time 0. Cells were harvested at different time points, and AHA incorporated protein was biotinylated as described in Materials and Methods. The Top1 synthesis ratio in the presence *vs* absence of 4-OHT was calculated to be 0.53±0.044. Met, methionine; bound, Streptavidin beads-bound fraction.

**Figure 5. Top1 knockdown enhances CSR in AER and splenic B cells. A.** The Top1 protein level in AER cells was measured by Western blot 48 hours after electroporation with

the indicated siRNA. **B.** Top1 knocked-down AER cells were stimulated with various concentrations of CIT (left) or 4-OHT (right) for 24 hours, and the surface IgA expression was quantified by flow cytometry. siRNAs used are as follows; closed circles, siTop1#33; squares, siTop#35; triangles, siAID; open circles, control. **C.** Knockdown of Top1 was performed in AER cells carrying the Tet-inducible microRNA (miR)-Top1 construct as described in Materials and Methods. The surface IgA expression was quantified by flow cytometry 24 hours after 4-OHT addition. Squares, miR-Top1; circles, miR-neg. (left) Cells were exposed to indicated concentrations of Tet for 24 hours, and then incubated with 1 μM of 4-OHT. Closed and open symbols, with and without 4-OHT, respectively. (right) Cells were initially exposed to 1 μg/ml doxycycline for 24 hours and then CSR was induced by indicated concentrations of 4-OHT. Closed and open symbols, with and without doxycycline, respectively. **D**. Top1 knockdown augmented CSR in splenic B cells. AIDER-induced CSR in the control siRNA- and Top1 siRNA(#33)-treated splenic B cells. $AID^{-/-}$ splenic cells were cultured for 24 hours after siRNA introduction and then infected by the AIDER-IRES-GFP retrovirus. The surface IgG1 and GFP levels were analyzed by flow cytometry 24 hours after 4-OHT addition. Numbers in the quadrants are the percentages of switched cells among the GFP positive population.

**Figure 6. Top1 knockdown alters the single-stranded area of the Sμ region. A.** Schematic representation of the PCR amplified sequence flanking the Sμ core region. Grey and black arrowheads indicate forward (bisulfite specific) and reverse primers, respectively. The C-rich (59 Cs) area (150 bp) was located at the 3' end of the amplified fragment (721 bp) and indicated by dotted line. **B.** The bisulfite reactivity of the 59 C bases, with or without Top1 knockdown in CH12F-3 cells. Each C base with its position number from the left end of the

721 bp amplified segment is indicated on horizontal axis and the percent converted at each position out of the total molecules analyzed is plotted on vertical axis. The three sensitive areas are indicated by horizontal bars labeled I, II and III. **C.** Summary of the total C to T conversion frequency.

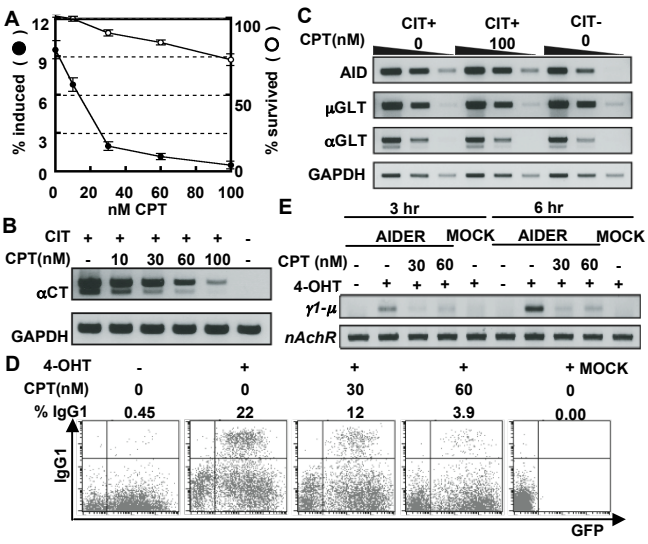
A
% induced ( ● )
% survived ( ○ )
nM CPT
B
CIT
CPT(nM)
αCT
GAPDH
C
CIT+ 0
CIT+ 100
CIT- 0
CPT(nM)
AID
μGLT
αGLT
GAPDH
D
4-OHT
CPT(nM)
% IgG1
0.45
22
12
3.9
0.00
+ MOCK
IgG1
GFP
E
3 hr
6 hr
AIDER
MOCK
CPT (nM)
4-OHT
γ1-μ
nAchR

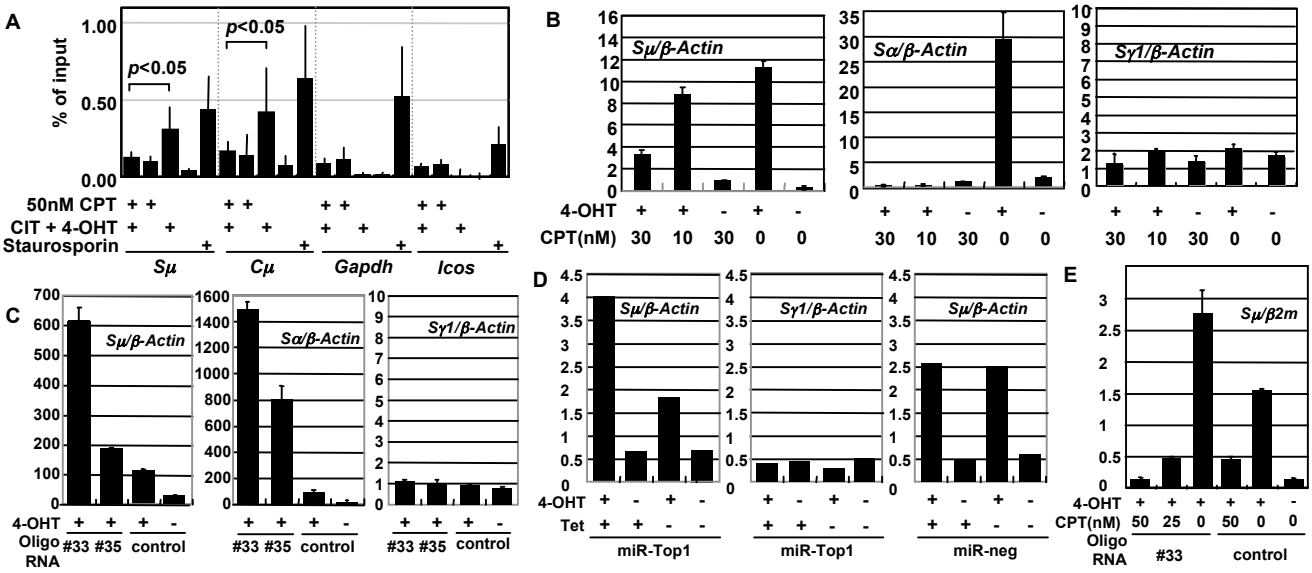
A
% of input
1.00
0.50
0.00
p<0.05
p<0.05
50nM CPT
CIT + 4-OHT
Staurosporin
Sμ
Cμ
Gapdh
Icos
B
Sμ/β-Actin
Sα/β-Actin
Sγ1/β-Actin
4-OHT
CPT(nM) 30 10 30 0 0
C
Sμ/β-Actin
Sα/β-Actin
Sγ1/β-Actin
4-OHT
Oligo
RNA
#33 #35 control
D
Sμ/β-Actin
Sγ1/β-Actin
Sμ/β-Actin
4-OHT
Tet
miR-Top1
miR-Top1
miR-neg
E
Sμ/β2m
4-OHT
CPT(nM) 50 25 0 50 0 0
Oligo
RNA
#33
control

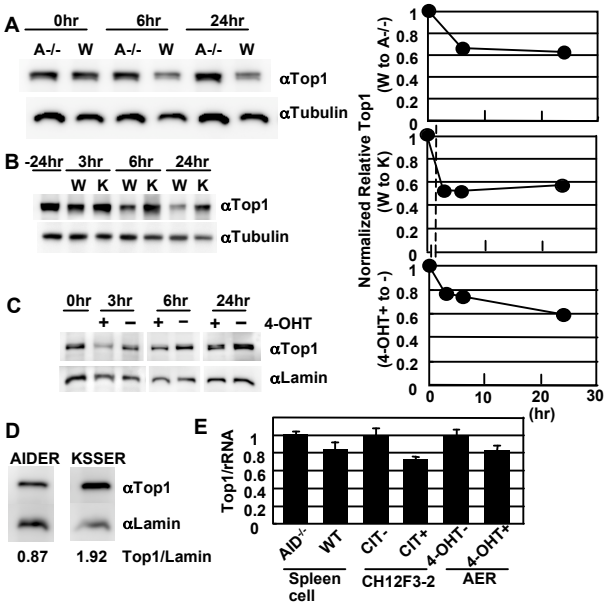
A
0hr
6hr
24hr
A-/- W A-/- W A-/- W
αTop1
αTubulin
B
-24hr 3hr 6hr 24hr
W K W K W K
αTop1
αTubulin
C
0hr 3hr 6hr 24hr
+ − + − + −
4-OHT
αTop1
αLamin
Normalized Relative Top1
(W to A-/-)
(W to K)
(4-OHT+ to -)
0 0.2 0.4 0.6 0.8 1
0 10 20 30
(hr)
D
AIDER KSSER
αTop1
αLamin
0.87 1.92 Top1/Lamin
E
Top1/rRNA
0 0.2 0.4 0.6 0.8 1
AID-/- WT CIT- CIT+ 4-OHT- 4-OHT+
Spleen cell
CH12F3-2
AER

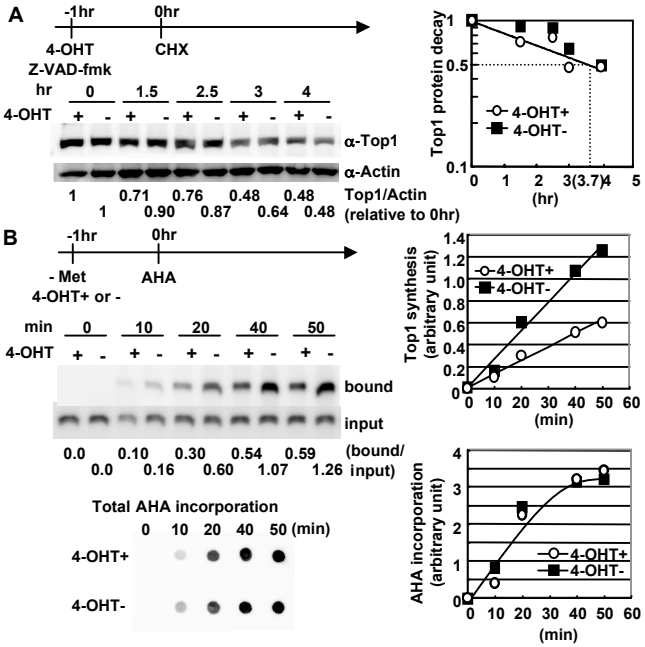
A
-1hr
0hr
4-OHT
CHX
Z-VAD-fmk
hr
0
1.5
2.5
3
4
4-OHT
+ - + - + - + - + -
α-Top1
α-Actin
1 0.71 0.76 0.48 0.48
1 0.90 0.87 0.64 0.48
Top1/Actin
(relative to 0hr)
Top1 protein decay
1
0.5
0.1
4-OHT+
4-OHT-
0 1 2 3(3.7)4 5
(hr)
B
-1hr
0hr
- Met
AHA
4-OHT+ or -
min
0
10
20
40
50
4-OHT
+ - + - + - + - + -
bound
input
0.0 0.10 0.30 0.54 0.59
0.0 0.16 0.60 1.07 1.26
(bound/
input)
Top1 synthesis
(arbitrary unit)
1.4
1.2
1.0
0.8
0.6
0.4
0.2
0
4-OHT+
4-OHT-
0 10 20 30 40 50 60
(min)
Total AHA incorporation
0 10 20 40 50 (min)
4-OHT+
4-OHT-
AHA incorporation
(arbitrary unit)
4
3
2
1
0
4-OHT+
4-OHT-
0 10 20 30 40 50 60
(min)

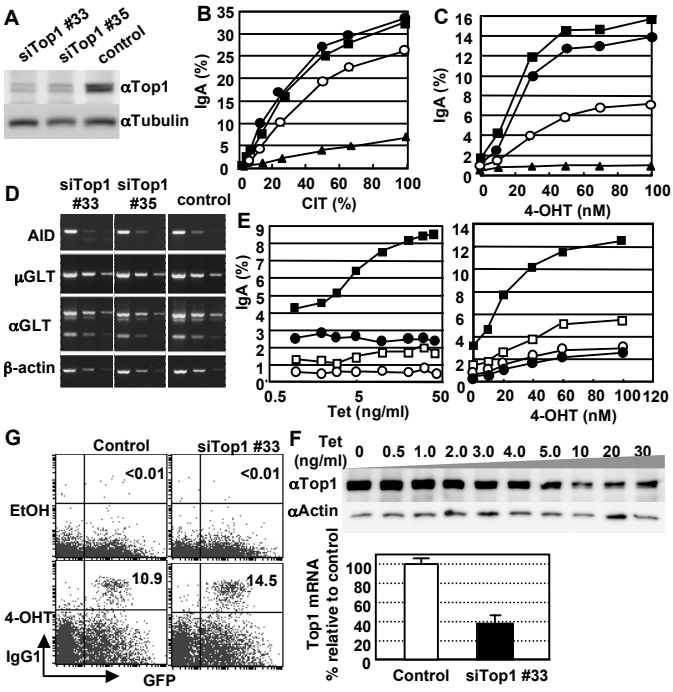
A
siTop1 #33
siTop1 #35
control
αTop1
αTubulin
B
IgA (%)
CIT (%)
C
IgA (%)
4-OHT (nM)
D
siTop1 #33
siTop1 #35
control
AID
μGLT
αGLT
β-actin
E
IgA (%)
Tet (ng/ml)
4-OHT (nM)
F
Tet (ng/ml)
0 0.5 1.0 2.0 3.0 4.0 5.0 10 20 30
αTop1
αActin
Top1 mRNA % relative to control
Control
siTop1 #33
G
Control
siTop1 #33
<0.01
<0.01
EtOH
10.9
14.5
4-OHT
IgG1
GFP

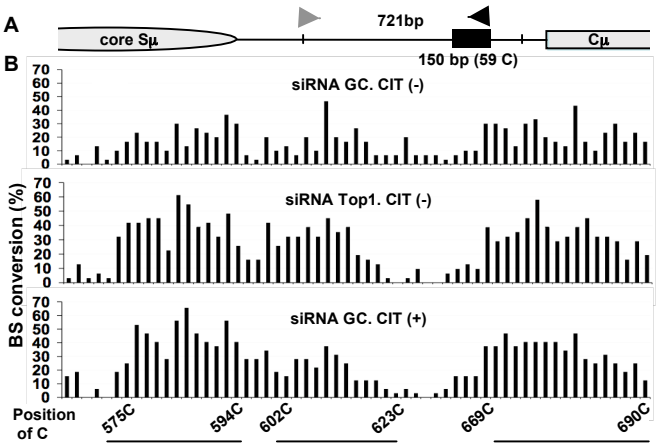


C

| siRNA | Stimulation by CIT | Clones | Total conversion | Conversion frequency | CSR (%) |
|---|---|---|---|---|---|
| Control | - | 31 | 300 | 16.2 | 0.5 |
| Top1 #33 | - | 30 | 496 | 27.1 | 1.2 |
| Control | + | 32 | 504 | 26.7 | 30.0 |

**Supplementary Information**

**Cell Culture and Stimulation**

CH12F3-2 cells were cultured and stimulated for class-switch induction as described previously (1). Red blood cell-depleted splenic B cells isolated using a B-cell isolation kit (Myltenyi Biotec) were obtained from 2-8-month-old wild-type or $AID^{-/-}$ mice on a C57BL6 background. The cells were cultured with LPS and IL4 as described previously (2).

**RT-PCR**

Total RNA was purified with TRIzol reagent (Invitrogen) and reverse-transcribed by the SuperScriptIII enzyme (Invitrogen) with an oligo(dT) primer. PCR for germline transcripts and AID mRNA detection was performed as described previously (3). For the αCTs, we used the reported primer set (4) and LA-Taq (Takara) for PCR amplification, which had an initial denaturing step of 94°C for 1 min followed by 35 cycles at 94°C for 30 sec, 61°C for 30 sec, and 72°C for 30 sec. GAPDH mRNA was detected as a positive control for RT-PCR. The RNA expression level of Top1, rRNA, endogenous AID, and μ- and α-GLT was quantified by ABI 7900 with each primer set. 18S rRNA TaqMan probe (ABI) or GAPDH primer set were used as internal control. The primer sets for μ- and α-GLT were described previously (4), and the others are shown in Table S2.

**DC-PCR**

Digestion circularization (DC)-PCR was done as described previously (5) with some modifications. Briefly, 100 ng of genomic DNA digested with EcoRI was subjected to a self-ligation reaction with T4 DNA ligase at 16°C overnight. Then, the circularized DNA was amplified for IgH genotyping by using AmpliTaq Gold enzyme with the primers described in Table S2. PCR amplification was done with an initial denaturing step of 94°C for 9 min followed by 40 cycles at 94°C for 30 sec and 65°C for 3 min.

**Materials and Animals**

The antibodies used for flow cytometric analysis by FACS Calibur (BD) were an FITC-conjugated anti-IgM antibody (eBioScience) and PE-conjugated anti-IgA antibody (eBioScience). Camptothecin (CPT) was purchased from Calbiochem and dissolved in dimethyl sulfoxide (DMSO). Anti-human Top1 monoclonal antibodies from Abnova and LifeSpan Biosciences were used to detect Top1 in the nucleoplasmic fraction of AER cells and in splenic B cells, respectively by Western blotting procedure(3). AID knockout mice (3) were maintained at the Institute of Laboratory Animals, Graduate School of Medicine, Kyoto University. Wild-type C57/BL6 mice

were purchased from CLEA Japan. Our experimental protocols using mice were approved by the Animal Research Committee, Graduate School of Medicine, Kyoto University. AID and its mutant constructs were previously described (6). Recombinant retrovirus was prepared and used to infect cells as described previously (2, 7).

**Nucleoplasm Fractionation**

The nucleoplasm fraction was isolated by the method described by Dieckmann (8) with minor modifications. Briefly, cells were washed with PBS three times. After suspension in hypotonic buffer with 4mM $Mg^{2+}$, triton X-100 was added to the suspension to 0.3%. Cells were homogenized and washed with 0.25M sucrose. Nuclei were collected, re-suspended in 0.34M sucrose, sonicated and centrifuged on 0.88M sucrose cussion to precipitate nucleoli. Supernatants were used as the nucleoplasmic fraction.

**CHIP Assay**

The CHIP experiment was done with anti-γH2AX antibody (JBW301) as described (9). Relative amounts of *Sμ, Cμ, Gapdh* and *Icos* regions in the precipitates were measured by real-time PCR with iQ™SYBR®Green Supermix (Bio-Rad). The values were calculated as a percent of the input. The *p* value obtained from the one-tailed paired Wilcoxon's *t*-test. Primers used for the real-time PCR are shown in Supplementary Table 2.

**Top1 Protein Decay Analysis**

z-VAD-FMK is purchased from Peptide Institute and cycloheximide (CHX) is from Nacalai tesque. The cells were lysed in RIPA buffer. Western blot with anti-Top1 or anti β-actin antibody was measured by NIH Image software (NIH) and plotted to the semi-logarithmic graph.

**References**


1. Nakamura M, *et al.* (1996) High frequency class switching of an IgM+ B lymphoma clone CH12F3 to IgA+ cells. *Int Immunol* 8:193-201.
2. Doi T, Kinoshita K, Ikegawa M, Muramatsu M, Honjo T (2003) De novo protein synthesis is required for the activation-induced cytidine deaminase function in class-switch recombination. *Proc Natl Acad Sci U S A* 100:2634-2638.
3. Muramatsu M, *et al.* (2000) Class switch recombination and hypermutation require activation-induced cytidine deaminase (AID), a potential RNA editing enzyme. *Cell* 102:553-563.
4. Kinoshita K, Harigai M, Fagarasan S, Muramatsu M, Honjo T (2001) A hallmark of active class switch recombination: transcripts directed by I promoters on looped-out circular DNAs. *Proc Natl Acad Sci U S A* 98:12620-12623.

5. Chu CC, Paul WE, Max EE (1992) Quantitation of immunoglobulin mu-gamma 1 heavy chain switch region recombination by a digestion-circularization polymerase chain reaction method. *Proc Natl Acad Sci U S A* 89:6978-6982.
6. Doi T, *et al.* (2009) The C-terminal region of activation-induced cytidine deaminase is responsible for a recombination function other than DNA cleavage in class switch recombination. *Proc Natl Acad Sci U S A* 106:2758-2763.
7. Fagarasan S, Kinoshita K, Muramatsu M, Ikuta K, Honjo T (2001) In situ class switching and differentiation to IgA-producing cells in the gut lamina propria. *Nature* 413:639-643.
8. Dieckmann R, Coute Y, Hochstrasser D, Diaz J-J, Sanchez J-C (2005) in *The Proteomics Protocols Handbook* (Humana Press Inc., Totowa, NJ), pp. 79-85.
9. Nagaoka H, Ito S, Muramatsu M, Nakata M, Honjo T (2005) DNA cleavage in immunoglobulin somatic hypermutation depends on de novo protein synthesis but not on uracil DNA glycosylase. *Proc Natl Acad Sci U S A* 102:2022-2027.

**Supporting Information Figure Legends**

**Figure S1.** Principle of DC-PCR. Arrows indicate the positions and directions of the primers.

**Figure S2. A high concentration of camptothecin (CPT) causes DNA break nonspecifically. A.** AER cells were treated with 150 nM or 50 nM CPT with or without 1 μM 4-OHT, for 16 hours. **B.** The same cells were treated with 50 nM CPT with or without 1 μM 4-OHT for 16 hours as well.

**Figure S3. The decrease in the Top1 protein amount in whole cell extract from AER cells after AID activation.** AER cells were stimulated with 1 μM of 4-OHT or CIT. After 24 or 48 hours, cells were harvested and whole cell extract was recovered with RIPA buffer with Benzonase nuclease. Western blot signal by each antibody was measured and Top1/Actin ratio was calculated. NS, non-stimulated AER cells.

**Figure S4.** No site specific editing on Top1 mRNA. To examine if AID edits Top1 mRNA, sequencing analysis was performed. CH12F3-2 cells expressing AIDER were treated with OHT for 12 hours. Total RNA was extracted by Trizol (Invitrogen) then Top1 cDNA was amplified by RT-PCR with PrimeStar® polymerase (Takara). The fragments were cloned into pBlueScript-SK vector at restriction enzyme sites placed in each amplification primer and sequenced. Shown is the combined result of four sequencing experiments in which four parts, designated as A to D regions, were

subjected to each analysis. The diagram shows the map of mouse Top1 cDNA with the position of the A-D regions below. The number represents a nucleotide position according to the c DNA sequence data of NM_009408. One arrow indicates one point mutation found in OHT treated samples. Total mutation numbers were summarized in the table. Sequence data from OHT non treated samples at regions A and D indicate the background level of this analysis. Primers used for cloning and sequencing were followings:

5’-ATGAATTCGCCCGCAGCGTTCGCACGCCGGCCGAC-3’;

5’-ATGGATCCATCATAGTAAAACTTGACACTCTCTGG-3’;

5’-ATGGATCCTTTTCACAGAACCCCTGCCGAGACTGG-3’;

5’-ATCAGAAGAGGAAGAGGATG-3’; 5’-GCATCAAATGGAAATTCCTAG-3’;

5’-CCAGTTCACGAATCAAGGGT-3’; 5’-TTCATTGATAAGCTTGCTCTG-3’;

5’-ACCATCCAATTCTGGGTGT-3’; 5’-GTGCCAATCGAGCTGTTGCA-3’;

5’-ATGGATCCAGTCTCGGCAGGGGTTCTGTGAAAAGG-3’;

5’-ATAAGCTTCGTTAAGTTGTAGGAGTTTATTTTAAA-3’.

**Figure S5. Reduced Top1 enhances R-loop and non-B DNA structure formation.** RNA polymerase II generates positive and negative supercoil in the front and rear, respectively, of the migrating transcriptional machinery. Negative supercoil in the rear may not be efficiently relaxed because of Top1 reduction and induce structural alterations including R-loop and non-B DNA.

**Figure S6. Non-B structure is prone to nicking by Top1.** Red (sense) and blue (anti-sense) strands forms cruciform structure. When Top1 encounters to the non-B structure it nicks DNA, however, cannot rotate DNA around helix and therefore fails to religate. Top1-DNA cleavage complex were cut out by the repair-related enzymes such as tyrosyl DNA phosphodiesterase/polynucletide kinase phosphatase. Thus irreversible cleavage is created by Top1.

**Figure S7. Top1 mRNA translation inhibition by an AID-edited microRNA.** Cytosine (C) of primitive-microRNA may be edited into uracil (U) by a complex of AID and its cofactors. Conversion from C to U will increase the correspondence of the miR to Top1 mRNA. Therefore, the processed and matured miR will suppress the translation of Top1.

**Fig. S1**

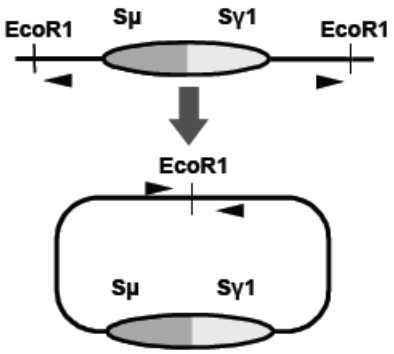

Fig. S2

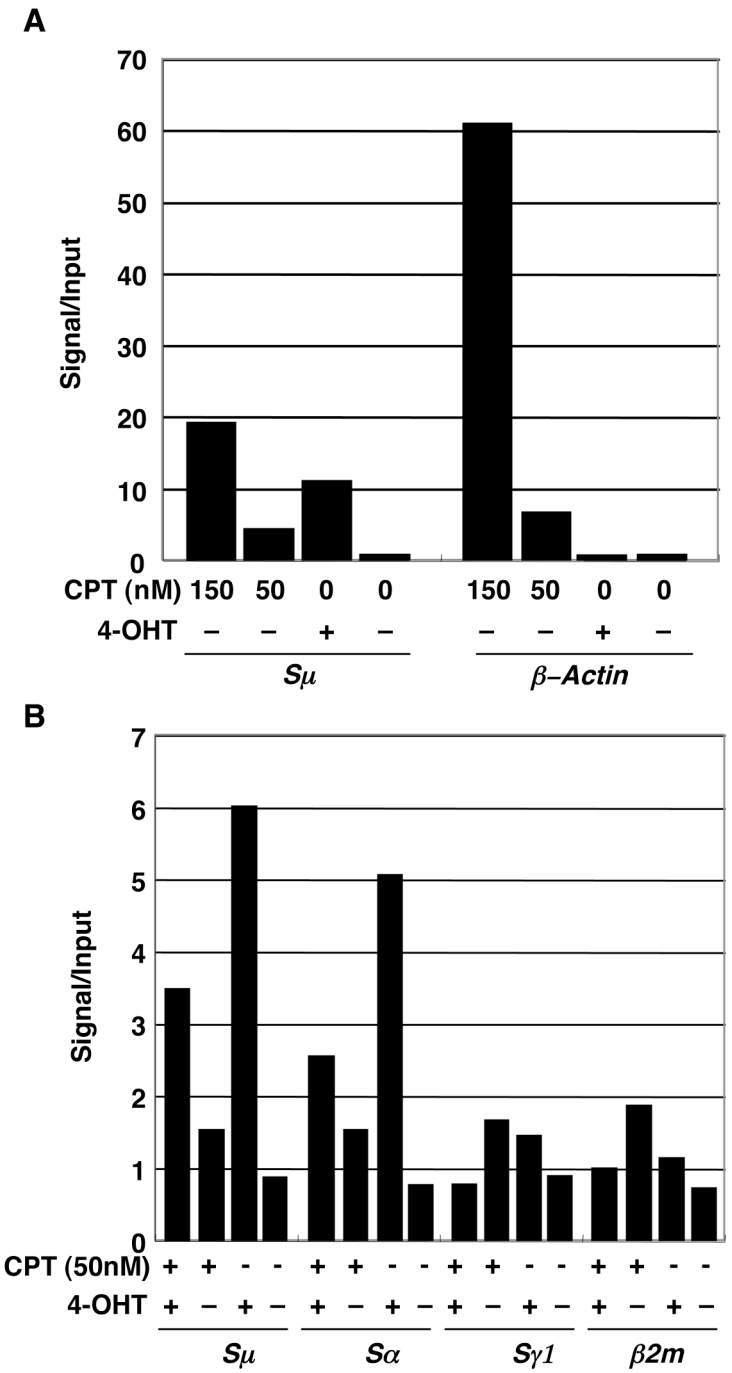
A
70
60
50
40
30
20
10
0
Signal/Input
CPT (nM) 150 50 0 0 150 50 0 0
4-OHT – – + – – – + –
Sμ
β–Actin
B
7
6
5
4
3
2
1
0
Signal/Input
CPT (50nM) + + - - + + - - + + - - + + - -
4-OHT + – + – + – + – + – + – + – + –
Sμ
Sα
Sγ1
β2m

Fig. S3

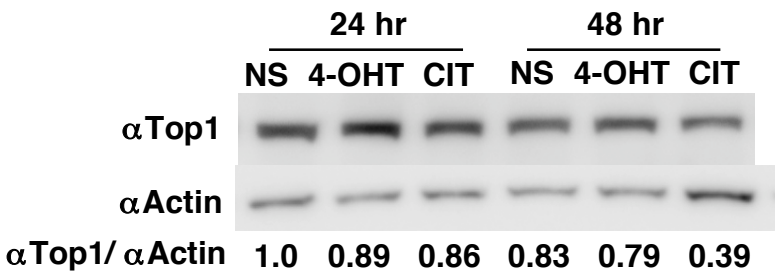
24 hr
48 hr
NS
4-OHT
CIT
NS
4-OHT
CIT
αTop1
αActin
αTop1/ αActin
1.0
0.89
0.86
0.83
0.79
0.39

**Fig. S4**

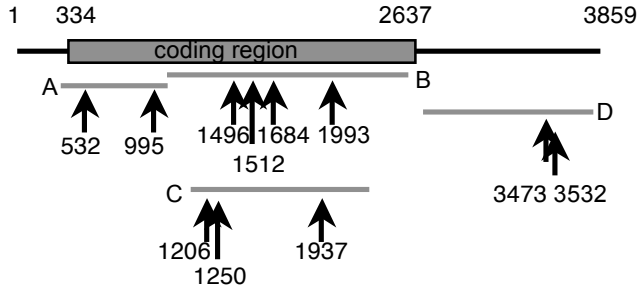


Number of point mutation found in each region

| | clone | sequence |
|---|---|---|
| | mutated/unmutated | mutation/bp |
| --(A region)-- | | |
| 4-OHT(+) | 2/79 | 2/55932 |
| 4-OHT(-) | 4/93 | 4/65844 |
| --(B region)-- | | |
| 4-OHT(+) | 4/47 | 4/75012 |
| --(C region)-- | | |
| 4-OHT(+) | 3/77 | 3/93940 |
| --(D region)-- | | |
| 4-OHT(+) | 2/39 | 2/45006 |
| 4-OHT(-) | 3/46 | 3/52946 |

Fig. S5

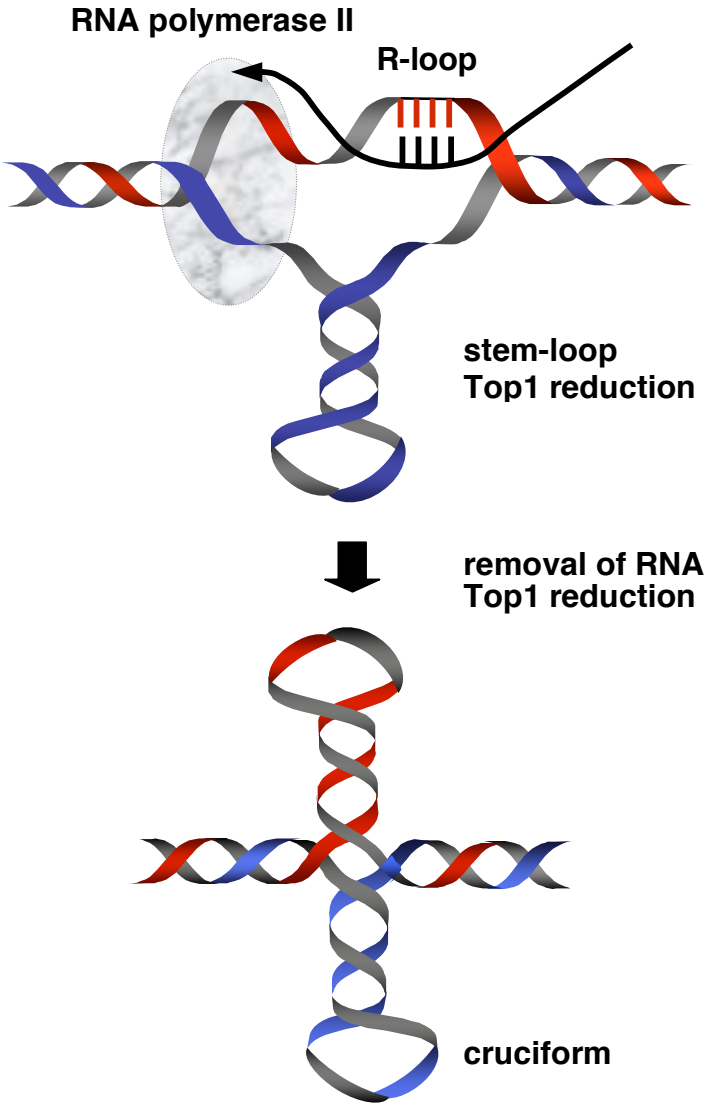
RNA polymerase II
R-loop
stem-loop
Top1 reduction
removal of RNA
Top1 reduction
cruciform

**Fig. S6**

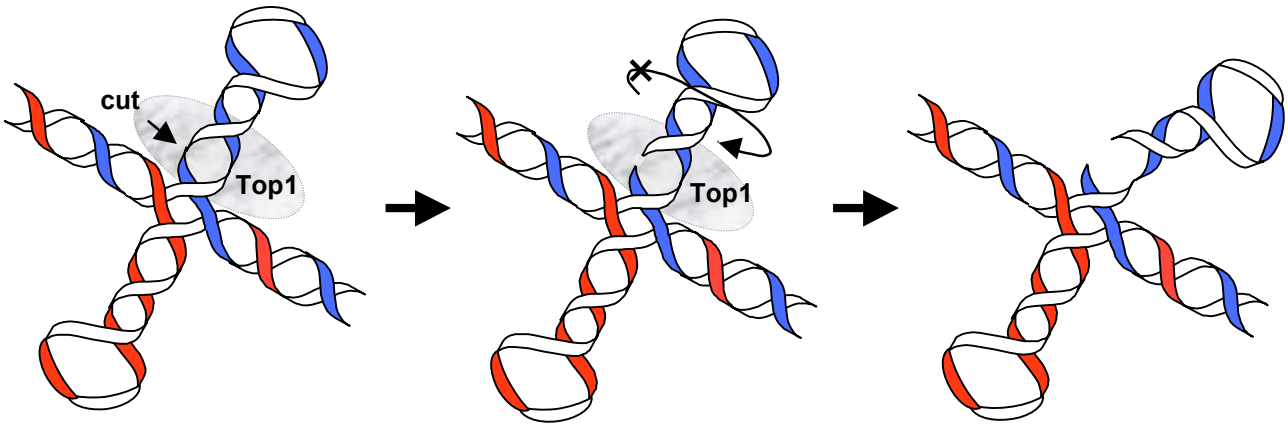


Nicking by Top1 | Inhibition of rotation | Removal of Top1

Fig. S7

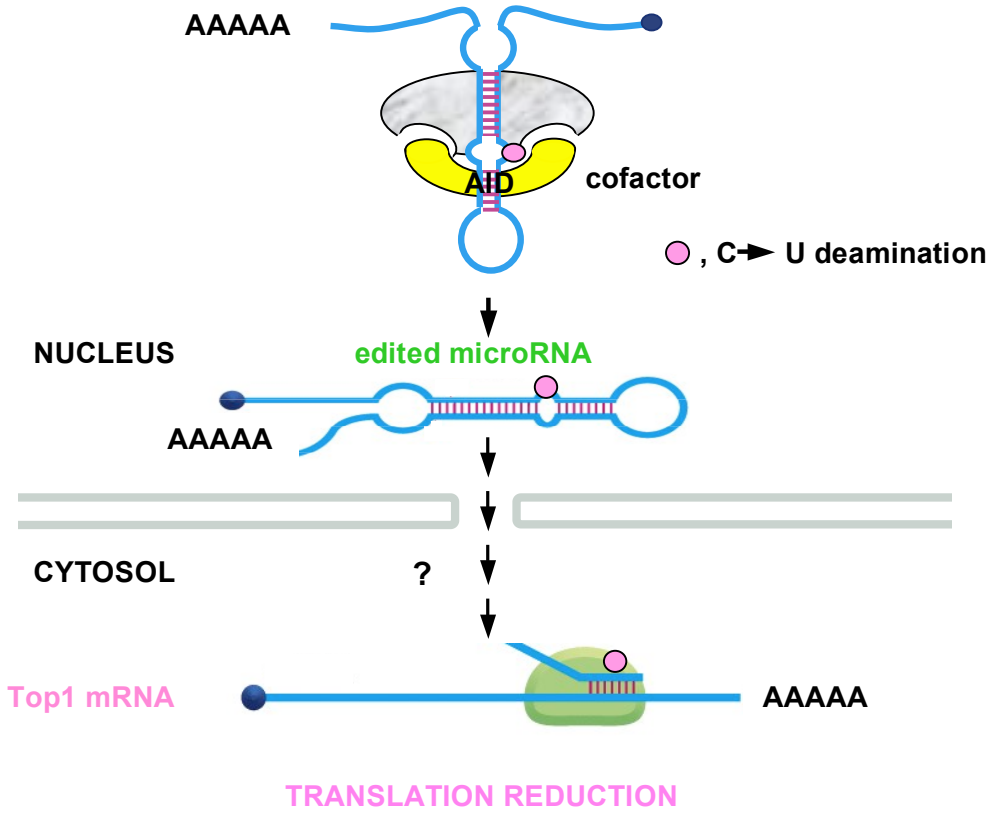
AAAAA
AID
cofactor
, C➔ U deamination
NUCLEUS
edited microRNA
AAAAA
CYTOSOL
?
Top1 mRNA
AAAAA
TRANSLATION REDUCTION

**Table S1. Inhibitors tested for CSR**

| Inhibitors | Targets | Effects on αCT |
|---|---|---|
| Etoposide VP16 (2μM) | Top2α | - |
| Merbarone (20μM) | Top2α | - |
| Doxorubicin (100nM) | Top2α | - |
| KU7026 (10μM) | DNA-PK | + |

AER cells, CH12F3-2 cell expressing AIDER were stimulated in the presence or absence of indicated inhibitors alpha circle transcripts were assayed by RT-PCR as described in Fig. 1B.

## Table S2. Nucleotide sequences of primers, oligo RNA, and linker

| | | |
|---|---|---|
| **Top1 knockdown RNA duplex** | | |
| #33 (Top1-MSS212033) | | UAU CAA UGA AGU ACA GUG CUA CAG C |
| #35 (Top1-MSS212033) | | CUU AGU AGU AUA UUC GUG GUC AAG C |
| **miR** | | |
| Top1 knockdown miR | | AA TTG CAA CAG CGA TTG GC |
| **DNA break assay** | | |
| biotinylated linker | top strand | biotin-ACA GGT TCA GAG TTC TAC AGT CCG AC |
| | bottom strand | phospho-GTC GGA CTG TAG AAC TCT GAA C |
| second linker | top strand | phospho-TCG TAT GCC GTC TTC TGC TTG |
| | bottom strand | CAA GCA GAA GAC GGC ATA CGA |
| amplification primers | forward | GTT CAG AGT TCT ACA GTC CGA |
| | reverse | CAA GCA GAA GAC GGC ATA CGA |
| gene-locus specific PCR primer sets | *Sμ* | Probe; FAM-CTA GTA AGC GAG GCT CT-MGB (ABI)<br>Primer; TGA TCA AAA TTA AGG GAA CAA GGT and TCA GAG AAG CCC ACC CAT CT |
| | *Sα* | Probe; FAM-GTG TCG TCT GAG CTG CAG AG-TAMRA (SIGMA)<br>Primer; ACA TGA TCAA CAG GCA CAA GG and GTC TCC TGT TGC TGC TTT CC |
| | *Sγ1* | Primer; CCTGAGCCCCGAGGATATC and AGTCCATGCCAAACA CATTCC |
| | *β2-Microglobulin (β2m)* | Probe; FAM- CTC GGT GAC CCT GGT CTT T-TAMRA (SIGMA)<br>Primer; CTG GCT GGC TCT CAT TTC AG and GGT CAG TGA GAC AAG CAC CA |
| | *β-Actin* | Probe; FAM-CCA CCA GGT AAG CAG GGA C -TAMRA (SIGMA)<br>Primer; CAG CTT CTT TGC AGC TCC TT and CTA GCC ACG AGA GAG CGA AG |
| **RT-PCR primer set** | | |
| Top1 | forward | TGC CTC CAT CAC ACT ACA GC |
| | reverse | CCC TTC GAG CAT CTG CTA AC |
| aicda 3'UTR | forward | GTG GCA TTC ACC TAT AGT TCC |
| | reverse | AGA ACC CAA TTC TGG CTG TG |
| β-actin | forward | ACTGGGACGACATGGAGAAG |
| | reverse | GGGGTGTTGAAGGTCTCAAA |
| gapdh | forward | AAAATGGTGAAGGTCGGTGT |
| | reverse | TGCCGTGAGTGGAGTCATAC |
| **DC-PCR primer set** | | |
| recombined | Iγ1 forward | GAGAGCAGGGTCTCCTGGGTAGG |
| | Iμ reverse | TGGAGACCAATAATCAGAGGGAAGA |
| Control | nAChRe1 | GGCCGGTCGACAGGCGCGCACTGACACCACTAAG |
| | nAChRe2 | GCGCCATCGATGGACTGCTGTGGGTTTCACCCAG |
| **Primers used for ChIP assay** | | |
| *Sμ* | forward | CCCAGCTTTGTGTGCTGATA |
| | reverse | GCTTCCCTCTGAGACACTGG |
| *Cμ* | forward | CTGTCGCAGAGATGAACCCCAATG |
| | reverse | ATCCTTTGTTCTCGATGGTCACCGG |
| *Gapdh* | forward | ATCCTGTAGGCCAGGTGATG |
| | reverse | GCTCAAGGGCTTTTAAGGCT |
| *Icos* | forward | CTGGGCCAGATGTGTTTTCT |
| | reverse | CCTGCCATGGTTTTTCTTGT |